Enthalpy Determinations on the Helium-Nitrogen System

DAVID T. MAGE and DONALD L. KATZ
University of Michigan, Ann Arbor, Michigan

Experimental isobaric heat capacity and differential latent heat measurements have been made on the helium-nitrogen system. Compositions studied were nominal 5, 25, 50, and 100% helium in nitrogen over the range 0 to 2,000 lb./sq.in.abs. and —250° to 50°F.

These data, combined with the previously reported work on nitrogen and the Joule-Thomson coefficients of Roebuck, are used to construct the complete pressure-enthalpy-composition network over the investigated limits of pressure and temperature.

The enthalpies obtained from experimental heat capacity and Joule-Thomson data are compared with enthalpies computed from PVT data. The changes of phase determined by differential latent heat measurements are compared with literature vapor-liquid equilibruim data.

This information is used to prepare pressure-enthalpy diagrams for all the mixtures investigated. A three-dimensional representation of the data on a pressure-enthalpy-composition diagram is presented. Constructions are outlined from which heats of mixing and partial molal enthalpies can be obtained.

The thermodynamic network developed is believed accurate within 1% and should be of use to those concerned with low-temperature separation of helium from nitrogen.

Accurate thermodynamic data are required for an economical process design for the separation of helium from natural gases. The data available from the literature consist of Joule-Thomson coefficients (*1*), PVTX data (*2* to *4*), and liquid-vapor equilibrium data (*5* to *13*). This research reports experimental isobaric enthalpy differences for the helium-nitrogen system over a temperature range of —250° to 50°F., and from 150 to 2,000 lb./sq.in.abs. These data are combined with the Joule-Thomson coefficients of Roebuck (*14*) to provide pressure-enthalpy diagrams for this system.

METHOD OF MEASUREMENTS

The equipment used to perform the enthalpy measurements reported here has been described previously (*15* to *19*). The flow calorimeter system utilizes a three-stage, oil-lubricated compressor for circulation. The compressed gas is cooled to the measuring conditions by a series of low-temperature baths cooled by dry ice and liquid nitrogen. The cooled gas enters a heat-shielded calorimeter in a constant-temperature bath where the heat capacity is measured. The pressure entering and leaving the calo-

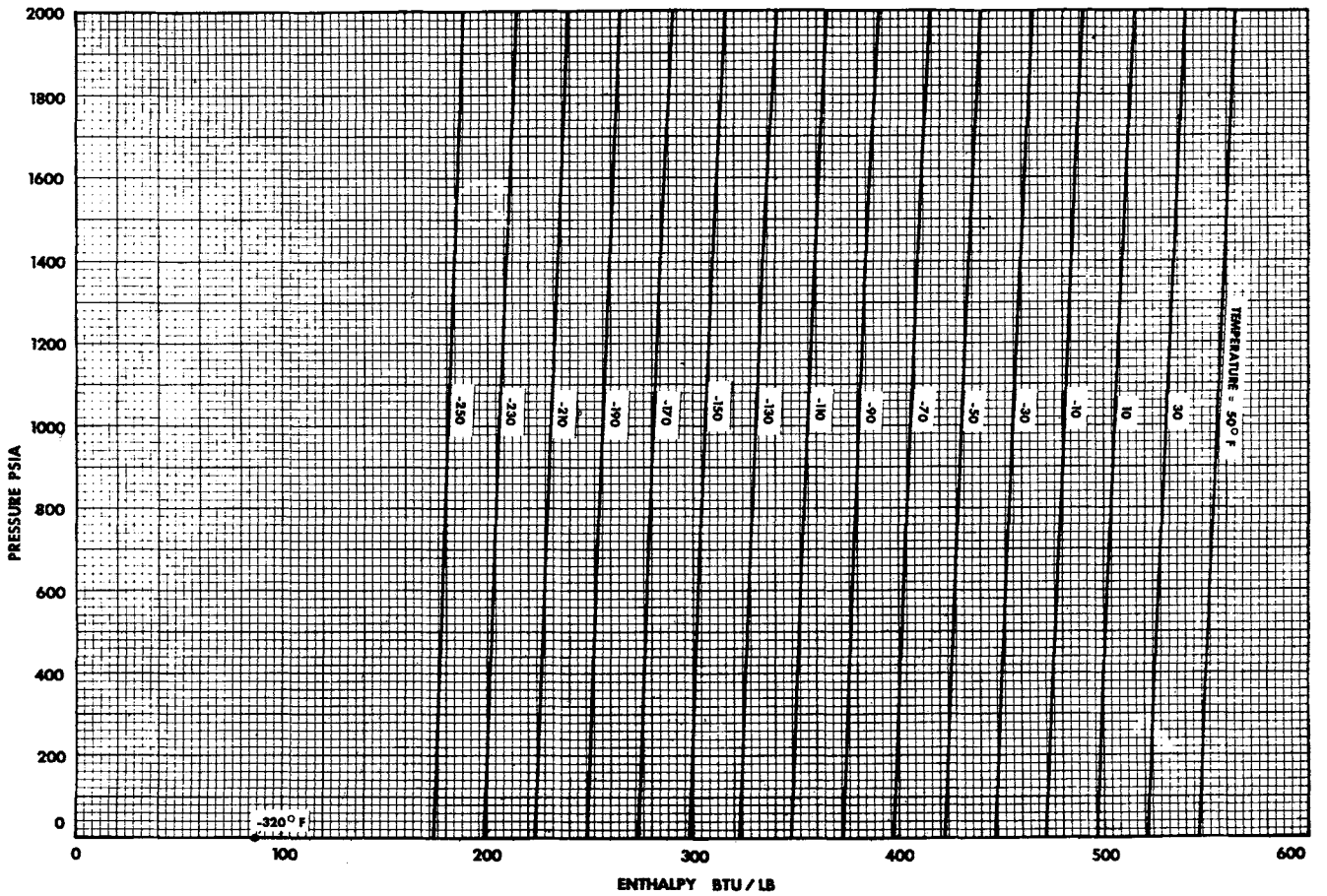

Fig. 1. Pressure—enthalpy diagram for helium.

TABLE 1. COMPOSITIONS OF MIXTURES INVESTIGATED WITH THE FLOW CALORIMETER

	Nominal % helium				
	0	5	25	50	100
Helium		5.0	24.6	49.9	99.99*
Nitrogen	99.95*	94.95*	75.33*	50.05*	0.005
Oxygen			0.02	0.01	
Argon	0.05	0.05	0.04	0.03	
Methane			0.01	0.01	0.005
Molecular weight	28.02	26.80	22.11	16.01	4.003

* These compositions were obtained by difference.

rimeter is measured and accurately controlled. The basic measurements involved are the mass flow rate, electrical power added to the fluid, and the resulting rise in temperature. Corrections are made for the pressure drop through the calorimeter, as well as heat leakage.

NITROGEN

Measurements on nitrogen performed at this laboratory have been reported (*20*).

HELIUM

Thermodynamic properties for gaseous helium reported in the literature consist of PVT data (*2* to *4*, *24* to *26*), isobaric specific heats (*27*, *28*), and the Joule-Thomson coefficients (*14*, *29*). These Joule-Thomson coefficients reported in the literature contain an error in that they are reported to be independent of pressure. The coefficients were independent of pressure on an isenthalp but not on an isotherm. Examination of Roebuck's original data (*30*) permitted all corrections to be made (*14*, *17a*).

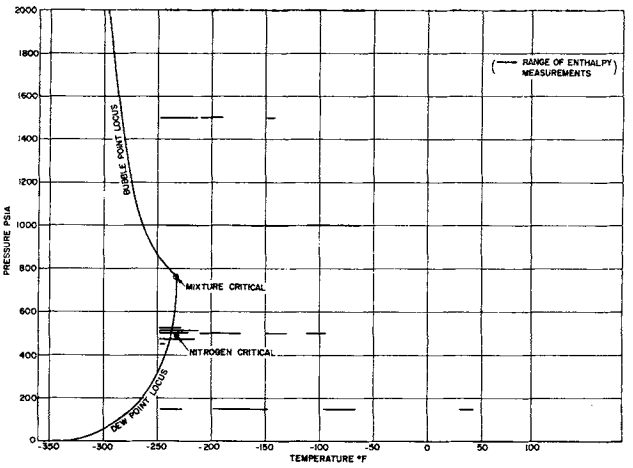

Fig. 2. Conditions of measurement for a 0.050 helium–0.950 nitrogen mixture.

Specific heat measurements were made on Grade A helium supplied by the U.S. Bureau of Mines. The total impurity in the flow system as measured by mass spectrometer was below 100 p.p.m. (Table 1).

Isobaric enthalpy differences of this research agree within 0.5% with values derived from the most recent enthalpy tabulations obtained from PVT data (*31*, *32*).

The pressure-enthalpy diagram (Figure 1) was constructed from the experimental data and selected literature values as follows. A reference state of 87 B.t.u./lb. was chosen at zero pressure and −320°F. This is also the enthalpy per pound of nitrogen at the same condition relative to $H = 0$ at −320.4°F. and 1 atm. in the saturated liquid state. The classical c_p value of $5/2(R)$ B.t.u./(lb.-mole)(°R.) was integrated at zero pressure to give the enthalpy at 30°F. (R = universal gas constant; c_p =

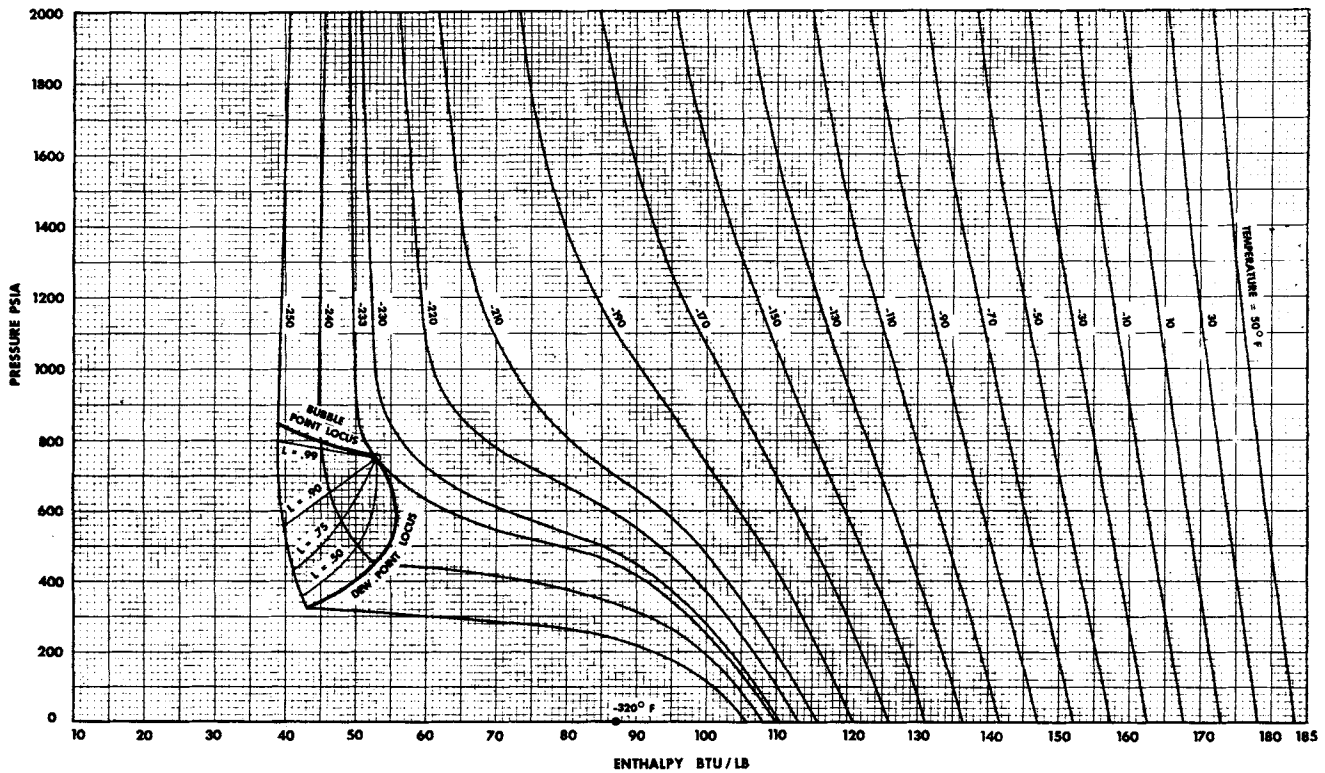

Fig. 3. Pressure–enthalpy diagram for a 0.050 helium–0.50 nitrogen mixture.

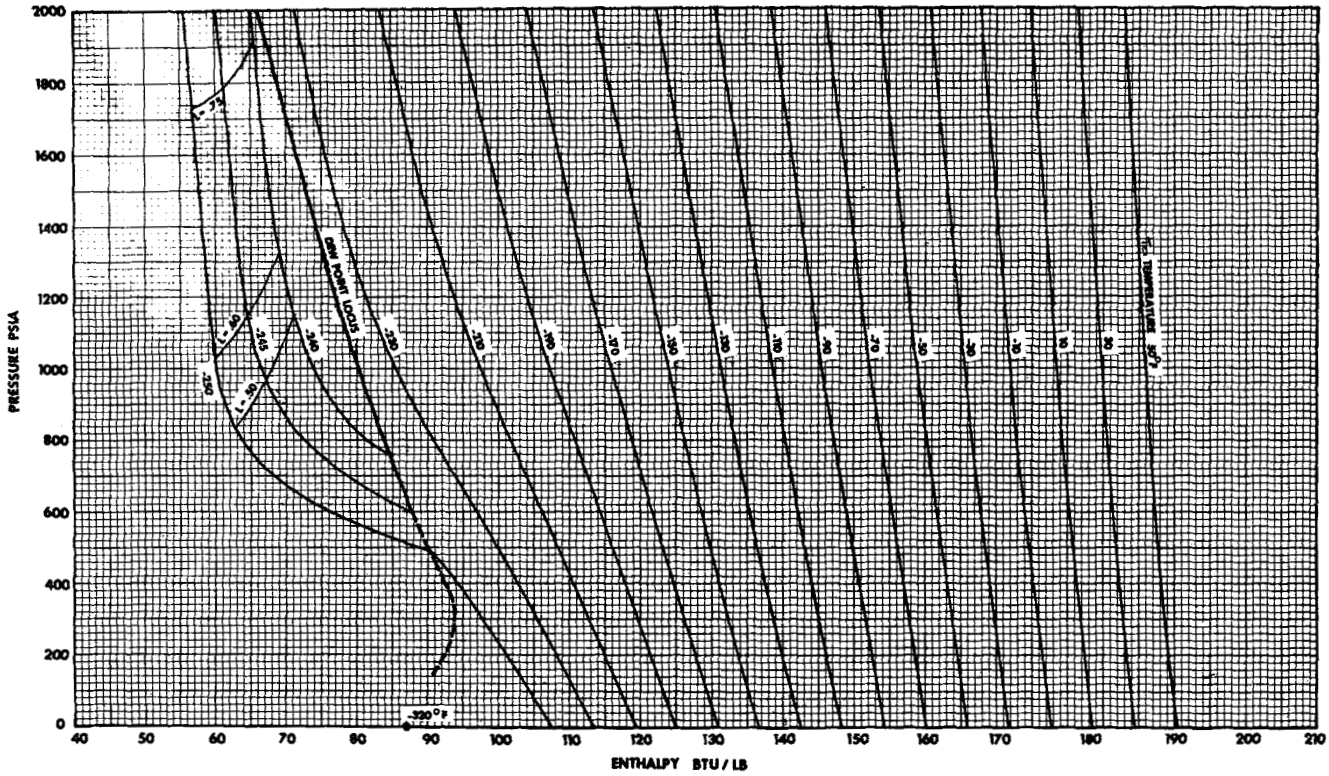

Fig. 4. Pressure–enthalpy diagram for a 0.246 helium–0.754 nitrogen mixture.

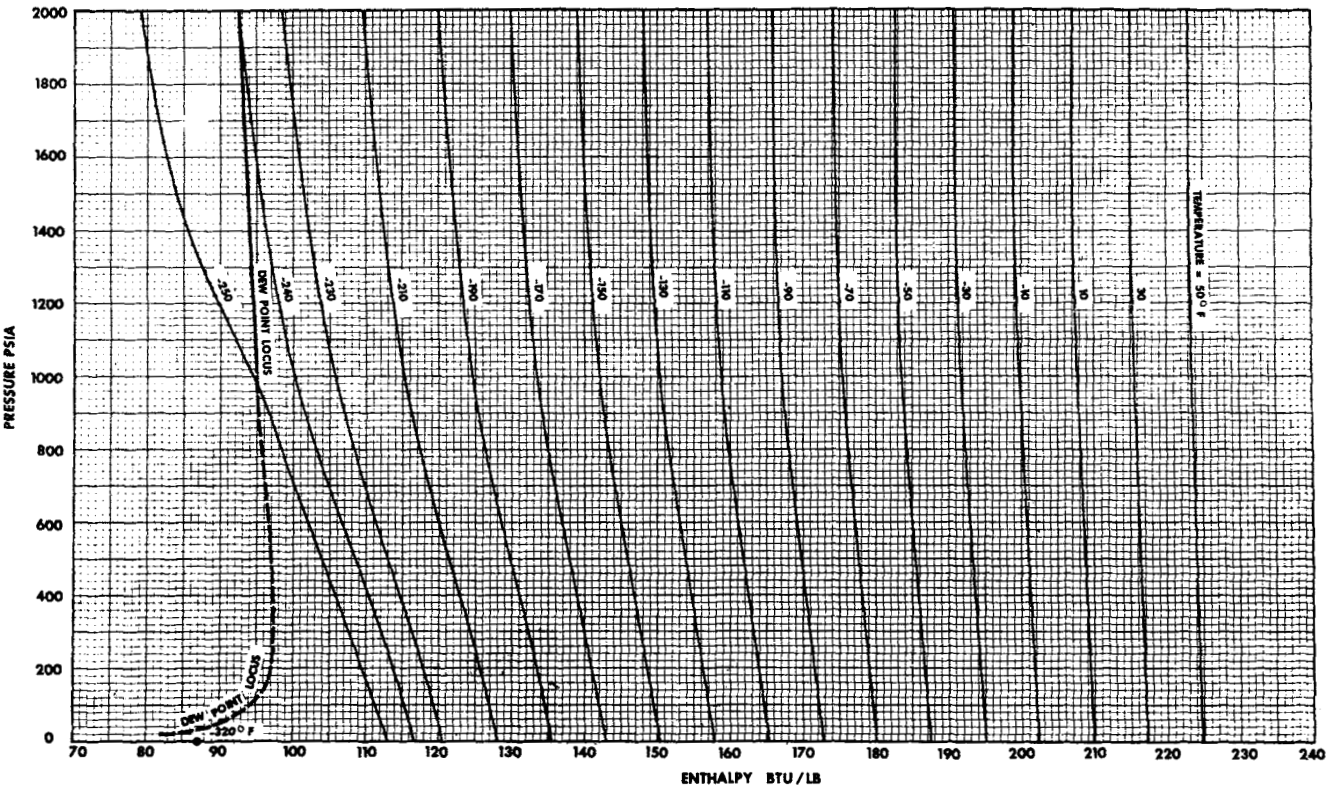

Fig. 5. Pressure–enthalpy diagram for a 0.499 helium–0.501 nitrogen mixture.

TABLE 2. SPECIFIC HEAT MEASUREMENTS FOR A 0.246 HELIUM-0.754 NITROGEN MIXTURE

Pressure, lb./sq. in. abs.	T_1, °F.	T_2, °F.	C_{p_m},* B.t.u./(lb.)(°F.)	Heat added, B.t.u./lb.
149.7	−23.89	+50.85	0.2946	22.01
149.6	−23.84	+47.15	0.2934	20.83
151.7	−245.77	−137.17	0.3153	34.24
151.7	−245.90	−207.92	0.3226	12.25
999.7	−246.19†	−241.73†	1.4032	6.26
999.7	−246.00†	−237.54†	1.5573	13.18
999.7	−245.75†	−223.56	1.1083	24.60
999.7	−245.64†	−234.10	1.4685	16.96
999.7	−246.40†	−217.40	1.0046	29.15

* C_{p_m} is mean heat capacity corrected for pressure drop.

† Temperature inside two-phase region.

isobaric heat capacity; μ = Joule-Thomson coefficient.) The product of c_p and μ was then integrated from 0 to 2,000 lb./sq.in.abs. at 30°F. The measured heat capacities, integrated between −250° and 50°F., were used to extend enthalpy at constant pressure over the complete range. This diagram is accurate to 1% over the complete range of pressure and temperature.

HELIUM-NITROGEN MIXTURES

The three mixtures investigated in the course of this research contained nominally 5, 25, and 50% helium in nitrogen (Table 1). Isobaric heat capacities and differential latent heats were measured for each of these three mixtures. Figure 2 indicates the conditions of measurement for the 5% helium mixture. The data on the 25 and 50% helium mixtures covered a similar range of pressure and temperature. Table 2 indicates how the original experimental data are reported (*17*).

The pressure-enthalpy diagrams (Figures 4, 5, and 6) were constructed in the following manner. An assumption of zero heat of mixing at 0 lb./sq.in.abs. and −320°F. was made. Since the enthalpies of both pure components are 87 B.t.u./lb. at this condition, the enthalpies for all of the mixtures at this condition remain at 87 B.t.u./lb. From the common reference state, the zero pressure heat capacities of the mixtures are integrated to 50°F. An integration of the product of Joule-Thomson and specific heat extended the enthalpy as a function of pressure to 2,000 lb./sq.in.abs. Integration of the experimental heat

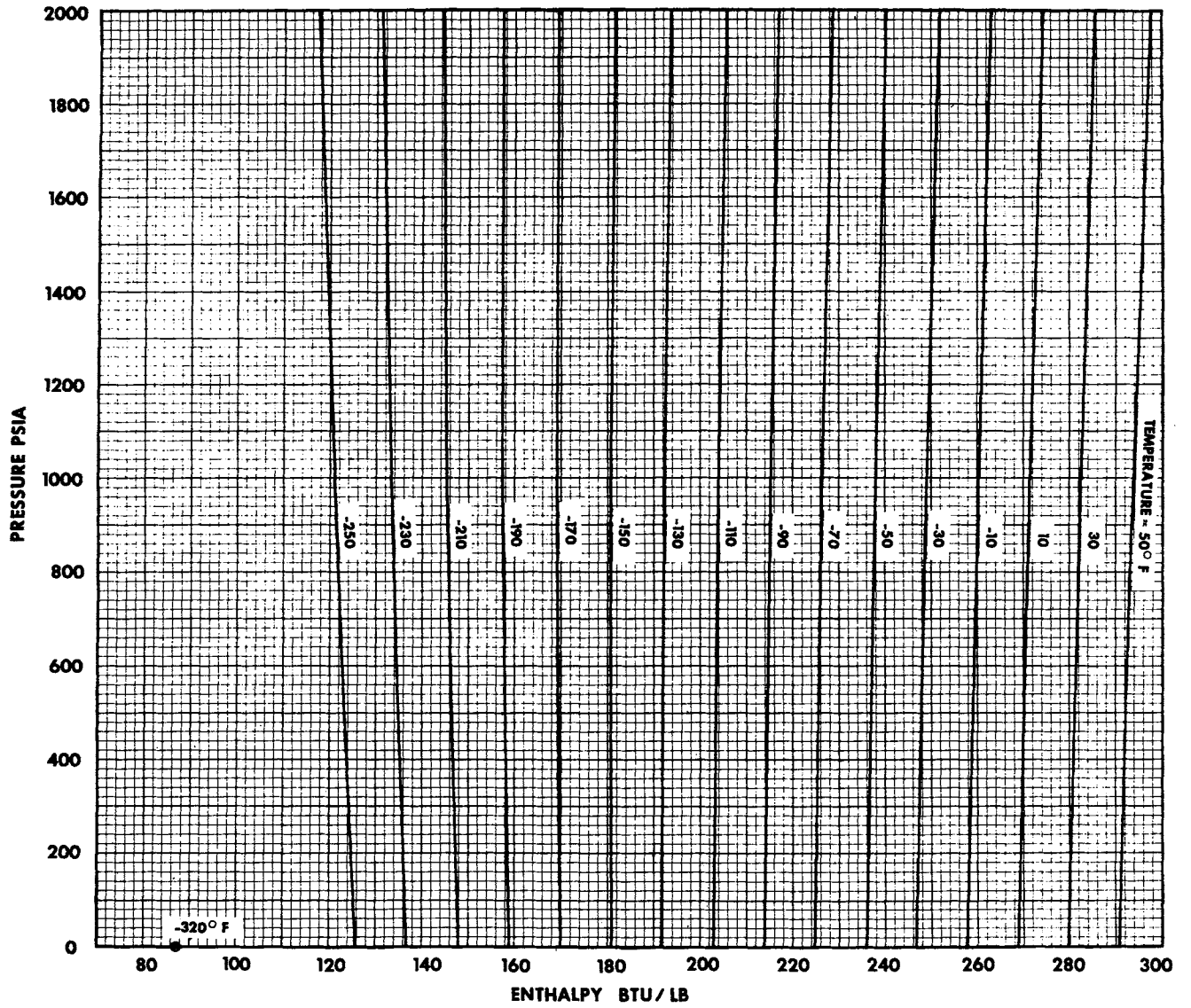

Fig. 6. Pressure–enthalpy diagram for a 0.755 helium–0.245 nitrogen mixture.

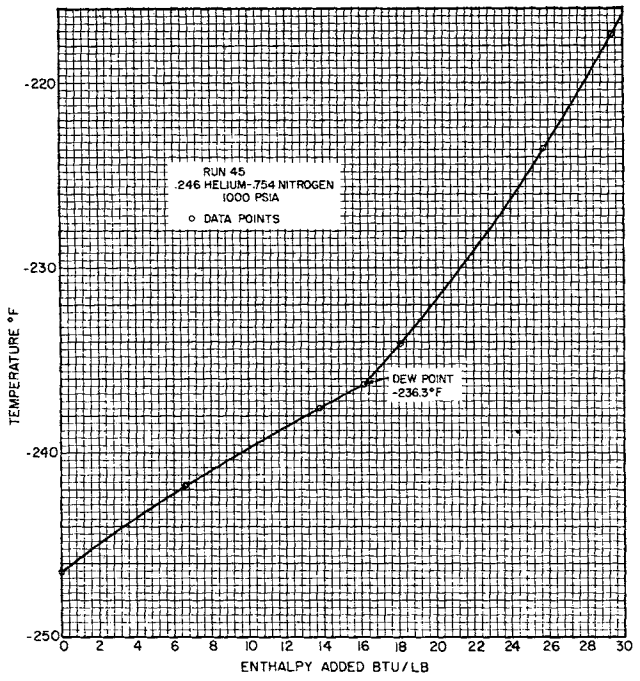

Fig. 7. Differential latent heat of a helium–nitrogen mixture.

capacities extended the enthalpy as a function of temperature from −250° to 50°F.

In addition to the three mixtures investigated, a pressure-enthalpy diagram (Figure 6) was prepared for a 75.5% helium in nitrogen mixture. The data used were from the isenthalps of Roebuck (*1*), combined with zero pressure heat capacities. The resulting series of charts allows a complete representation of the mixture enthalpies as a function of composition.

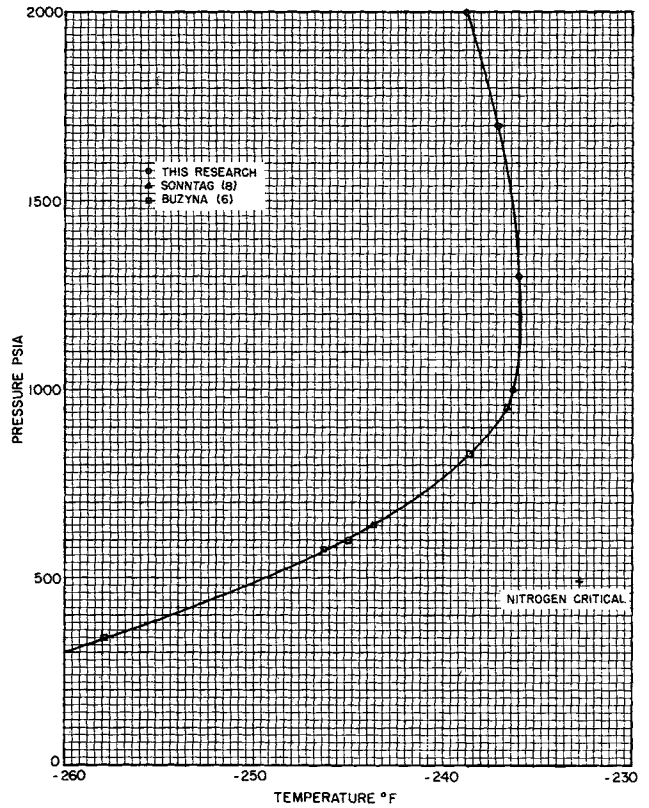

Fig. 8. Dew point locus of a 0.246 helium–0.754 nitrogen mixture.

COMPARISONS WITH THE LITERATURE

Phase equilibrium data derived from the enthalpy measurements as well as data available from the literature (*6* to *8*) were used to construct the two-phase regions and lines of constant liquid fraction. Figure 7 represents a differential latent heat of a 24.6% helium in nitrogen mixture at 1,000 lb./sq.in.abs. The data for this determination are presented in Table 2. The break in slope corresponding to the dew point for the mixture occurs at −236.3°F. Figure 8 compares the phase equilibrium data derived from enthalpy data of this research with recently reported vapor-liquid equilibrium data for the same system. In general, the agreement is within 0.2°F. of the literature values.

No heat capacity data on helium-nitrogen mixtures under pressure are available from the literature. Consequently, to make comparisons, we must relate the data of this research to values derived from treatment of PVTX data. Figure 9 compares isobaric enthalpy change data of this research with results obtained from the tabulation of Pfenning (32). Figure 10 compares the isothermal enthalpy change with values derived from Pfenning's tabulation (32). As would be expected, the values derived from PVTX data agree at high temperatures within 1%. As Pfenning's lower limit of −220°F. is approached, the deviations become on the order of 2%. For nitrogen, in the range of −250° to −220°F., deviations as high as 7% exist between the results of this research and two recent tabulations of enthalpy derived from PVTX data (*33, 34*). This deviation is not unexpected in view of the sensitivity of the PVT behavior in the crucial region and the magnification of error in the differentiation process.

Figure 11 shows a pressure–enthalpy–composition diagram at −250°F. The liquid-vapor region is the section of the surface between the dew point and bubble point loci. An interesting property of this diagram is that isobars connecting the dew points and bubble points must be straight lines, as there can be no heat of mixing be-

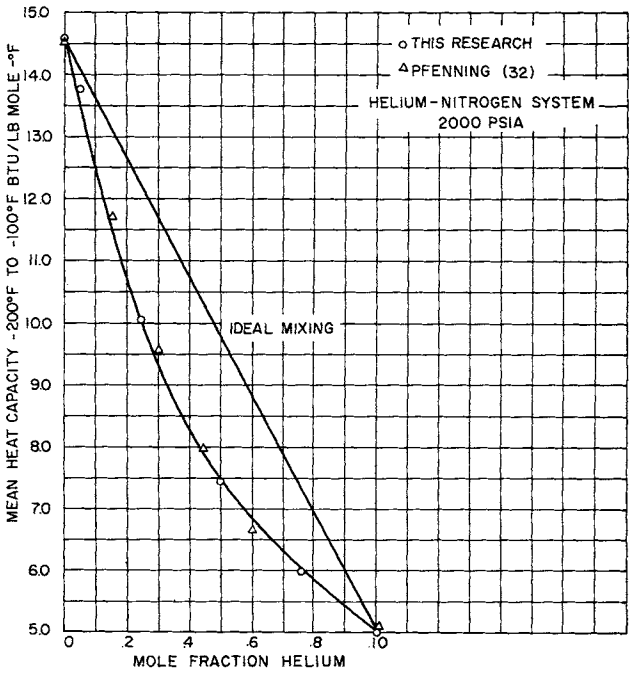

Fig. 9. Effect of composition on isobaric enthalpy change at low temperature.

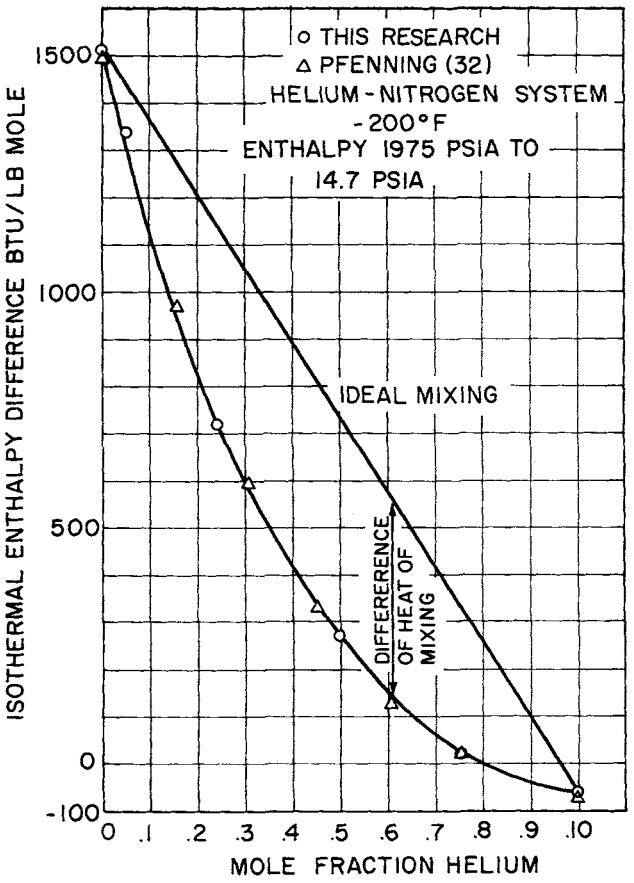

Fig. 10. Effect of composition on isothermal enthalpy change at low temperature.

tween saturated phases of a mixture. By drawing straight lines from the helium plane to the nitrogen plane, the heat of mixing can be obtained as the difference in enthalpy between the real mixture and an ideal mixture, represented by the straight line.

Figure 12 shows the heat of mixing at 2,000 lb./sq. in. abs. and −150°F. derived in this manner as a function of composition. A tangent to the curve will permit the

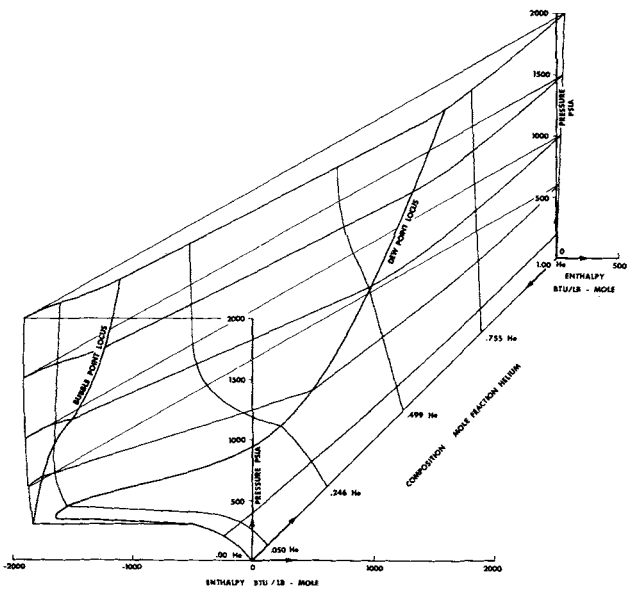

Fig. 11. Pressure enthalpy composition diagram for helium–nitrogen at −250°F.

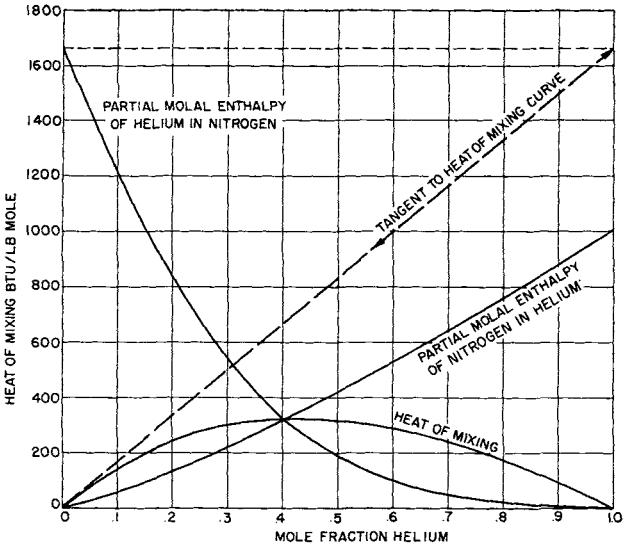

Fig. 12. Heat of mixing and partial molal enthalpies for helium–nitrogen at −150°F. and 2,000 lb./sq.in.abs.

calculation of the partial molal enthalpy of a component in the mixture relative to its pure component state at the identical condition.

In the construction of the thermodynamic charts, several independent paths, utilizing the heat capacity and Joule-Thomson data, arrived at the same answer, indicating a high degree of compatibility and consistency between the results of this research and those of Roebuck.

The combination of the results of this research and those of Roebuck establishes a consistent thermodynamic network for the helium–nitrogen system, and illustrates the present degrees of reliability between derived and experimental data above the critical temperature.

ACKNOWLEDGMENTS

The authors acknowledge the National Science Foundation, American Chemical Society Petroleum Research Fund, and Natural Gas Processors Association for research fellowships, and the U.S. Bureau of Mines, Helium Research Center for a gift of a large quantity of pure helium. We thank Professors John E. Powers and Joseph J. Martin for discussion of the theoretical implications of the data, Professor John R. Roebuck for the gift of equipment and his complete set of experimental records to the University of Michigan, and Edgar A. Manker and Alan E. Mather for help in the taking of the experimental data.

LITERATURE CITED

1. Roebuck, J. R., and Harold Osterberg, *J. Am. Chem. Soc.*, **60**, 341 (1938).
2. Kramer, G. M., and J. G. Miller, *J. Phys. Chem.*, **61**, 785 (1957).
3. Canfield, F. D., Jr., Ph.D. thesis, Rice Univ., Houston, Tex. (1962).
4. Miller, J. E., L. W. Brandt, and Lowell Stroud, *U.S. Bur. Mines R. I. 5845* (1961).
5. Burch, R. J., *J. Chem. Eng. Data*, **9**, 19 (1964).
6. Buzyna, G., R. A. MacRiss, and R. T. Ellington, *Chem. Eng. Progr. Symposium Series No. 44*, **59**, 101 (1963).
7. DeVaney, W. E., B. J. Dalton, and J. C. Meeks, Jr., *J. Chem. Eng. Data*, **8**, 473 (1963).
8. Sonntag, R. E., personal communication (1964).
9. Boone, W. J., W. E. DeVaney, and Lowell Stroud, *U.S. Bur. Mines R. I. 6178* (1963).
10. Mullins, P. V., *Chem. Eng. Progr.*, **44**, 567 (1948).
11. Brandt, L. W., Lowell Stroud, and J. E. Miller, *J. Chem. Eng. Data*, **6** (1961).

12. Brown, G. M., and L. F. Stutzman, *Chem. Eng. Progr.*, **45**, 142 (1949).
13. Davis, P. C., A. F. Bertuzzi, R. L. Gore, and Frederick Kurata, *Am. Soc. Mech. Engrs. Trans.*, **201**, 245 (1954).
14. "Smithsonian Physical Tables," Publ. 4169, Smithsonian Inst., Washington, D. C. (1954).
15. Faulkner, R. C., Ph.D. thesis, Univ. Michigan, Ann Arbor (1959).
16. Jones, M. L., Jr., Ph.D. thesis, Univ. Michigan, Ann Arbor (1961).
17. Mage, D. T., Ph.D. thesis, Univ. Michigan, Ann Arbor (1964).
17a. ———, *J. Chem. Phys.*, **42**, 2977 (1965).
18. Jones, M. L., Jr., D. T. Mage, R. C. Faulkner, and D. L. Katz, *Chem. Eng. Progr. Symposium Ser. No. 44*, **59**, 52 (1963).
19. Manker, E. A., D. T. Mage, A. E. Mather, J. E. Powers, and D. L. Katz, *Proc. Natl. Gas Proc. Assoc.*, 3 (1964).
20. Mage, D. T., M. L. Jones, Jr., D. L. Katz, and J. R. Roebuck, *Chem. Eng. Progr. Symposium Ser. No. 44*, **59**, 61 (1963).
21. Goff, J. A., and Serge Gratch, *Trans. Am. Soc. Mech. Engrs.*, **72**, 741 (1950).
22. Friedman, A. S., and David White, *J. Am. Chem. Soc.*, **72**, 3931 (1952).
23. ———, and H. L. Johnston, unpublished data.
24. Schneider, W. G., *Can. J. Res.*, **27B**, 4, 339 (1949).
25. Pfefferle, W. C., Jr., J. A. Goff, and J. G. Miller, *J. Chem. Phys.*, **23**, 509 (1955).
26. Michels, A., and H. Wouters, *Physica*, **8**, 923 (1941).
27. Scheel, K., and W. Heuse, *Ann. Phys.*, **40**, 473 (1913).
28. *Ibid.*, **37**, 79 (1912).
29. Roebuck, J. R., and Harold Osterberg, *Phys. Rev.*, **43**, 60 (1933).
30. Roebuck, J. R., collection of experimental records donated to Univ. Michigan Library.
31. Mann, D. B., *U.S. Natl. Bur. Stds. Tech. Note 154A* (1962).
32. Pfenning, D. B., J. B. Canfield, and Riki Kobayashi, *J. Chem. Eng. Data*, **10**, 9 (1965).
33. Bloomer, O. T., and K. N. Rao, *Inst. Gas. Technol. Res. Bull.* **18**, (1952).
34. Strobridge, T. R., *U.S. Natl. Bur. Stds. Tech. Note 129A* (1962).

Manuscript received March 9, 1965; revision received September 9, 1965; paper accepted September 9, 1965. Paper presented at A.I.Ch.E. San Francisco meeting.

The Time-Optimal Control of Discrete-Time Linear Systems with Bounded Controls

HERBERT A. LESSER and LEON LAPIDUS

Princeton University, Princeton, New Jersey

The discrete-time, time-optimal control of high-order, linear systems with bounded controls is formulated as a problem in linear programming. The solution obtained requires a certain minimum number of controls to be on their bounds. Numerical results are obtained for a system with controls bounded on one and both sides and extensions indicated for state variable constraints. The method proves to be extremely fast and simple to solve on a high-speed digital computer.

In recent years there has been considerable interest in the optimal control of dynamic systems with much of the work to date being based on dynamic programming (*1*) or the maximum principle (*12, 14*). Proposed methods for obtaining solutions often work well for simple systems, but numerical difficulties are frequently encountered in deriving the optimal control of systems which are either highly nonlinear or of high order.

This paper describes the first phase of a study (9) of the time-optimal control of high-order, linear systems with bounded controls. This particular phase of the study treated discrete-time (sampled data) systems, that is, systems whose control variables may be changed at the discrete times $k\Delta t$, $k = 1, 2, \ldots$ but must be held constant for $k\Delta t < t < (k + 1)\Delta t$, $k = 0, 1, 2, \ldots$. The time increment Δt is called the *sampling period.* It is desired to find that sequence of controls which will bring the system from its initial state to some desired state in a minimum number of sampling periods.

The control of high-order systems is especially important in the chemical process industries where most of the process systems have either a large number of state

Herbert A. Lesser is with Esso Production Research Company, Houston, Texas.